TR-2007-05

Use of the Implicit HHT-I3 and the Explicit ADAMS Methods with the Absolute Nodal Coordinate Formulation

Bassam Hussein, Dan Negrut, Ahmed A. Shabana

August 2007

Abstract

This investigation is concerned with the use of an implicit integration method with adjustable numerical damping properties in the simulations of flexible multibody systems. The flexible bodies in the system are modeled using the finite element absolute nodal coordinate formulation (ANCF), which can be used in the simulation of large deformations and rotations of flexible bodies. This formulation, when used with the general continuum mechanics theory, leads to displacement modes, such as Poisson modes, that couple the cross section deformations, and bending and extension of structural elements such as beams. While these modes can be significant in the case of large deformations, and they have no significant effect on the CPU time for very flexible bodies; in the case of thin and stiff structures, the ANCF coupled deformation modes can be associated with very high frequencies that can be a source of numerical problems when explicit integration methods are used. The implicit integration method used in this investigation is the Hilber-Hughes-Taylor method applied in the context of Index 3 differential-algebraic equations (HHT-I3). The results obtained using this integration method are compared with the results obtained using an explicit Adams-predictor-corrector method, which has no numerical damping. Numerical examples that include bodies with different degrees of flexibility are solved in order to examine the performance of the HHT-I3 implicit integration method when the finite element absolute nodal coordinate formulation is used. The results obtained in this study show that, for very flexible structures, there is no significant difference in accuracy and CPU time between the solutions obtained using the implicit and explicit integrators. As the stiffness increases, the effect of some ANCF coupled deformation modes becomes more significant, leading to a stiff system of equations. The resulting high frequencies are filtered out when the HHT-I3 integrator is used due to its numerical damping properties. The results of this study also show that the CPU time associated with the HHT-I3 integrator does not change significantly when the stiffness of the bodies increases, while in the case of the explicit Adams method the CPU time increases exponentially. The fundamental differences between the solution procedures used with the implicit and explicit integrations are also discussed in this paper.

Contents

1. Introduction

The integration of large deformation finite element and multibody system algorithms is necessary in order to be able to solve many engineering and physics problems. One approach that bears potential for the successful integration of large deformation finite element and multibody system algorithms is based on the *absolute nodal coordinate formulation* (ANCF) (Dmitrochenko and Pogorelov, 2003; Garcia-Vallejo et al., 2003 and 2004; Shabana, 2005; Sopanen and Mikkola, 2003; Takahashi and Shimizu, 1999; Yoo et al., 2004). This formulation, which results in a constant mass matrix and zero Coriolis and centrifugal forces, leads to displacement modes, including Poisson modes, which couple the cross section deformations, and bending and extension of structural finite elements such as beams and plates (Hussein et al., 2007; Schwab and Meijaard, 2005). These coupled deformation modes can not be captured using other existing finite beam elements which are based on formulations that assume that the cross section remains rigid. The ANCF coupled deformation modes can be significant in the case of large deformations of very flexible structures. In this case, these coupled deformation modes are not associated with very high frequencies, and therefore, having these modes in the dynamic models does not lead to numerical problems and does not negatively impact the efficiency of the ANCF solution algorithm. In this case, little advantage can be achieved by using implicit integration as compared to explicit integration methods.

In the case of small deformations of stiff structures in multibody system applications, the finite element floating frame of reference formulation, that can be used to systematically eliminate high frequency modes, can be employed. On the other hand, in the case of large deformations of stiff structures, the floating frame of reference formulation can not be used if the deformation of the structural components assumes a complex shape. Attempts have been recently made in several investigations to use the absolute nodal coordinate formulation to solve large deformation problems in the case of stiff structures. In this case, the ANCF coupled deformation modes are associated with high frequencies, resulting in a stiff system of dynamic equations. Explicit integration methods can be very inefficient or even fail when they are used to solve the resulting system of stiff dynamic equations. For such a stiff system, implicit integration methods are known to be much more efficient than explicit methods. As the frequency increases, an explicit integrator selects a smaller step size in order to be able to capture the high frequency oscillations in the solution. The decrease in the step size leads to an increase in the number of function evaluations with an overall increase in the CPU time. Furthermore, the step size required to capture the high frequency oscillations may become less than the integrator specified limit value leading to a termination of the simulation.

Implicit integrators, on the other hand, do not trace high frequency oscillations which can have negligible effect on the solution accuracy. For this reason, implicit integrators can take a much larger step size in the case of stiff systems, and can have better performance in the simulation of many multibody system applications as compared to the explicit integrators. Furthermore, some implicit integrators introduce, in a controllable fashion, numerical damping that results in filtering out of the small amplitude high frequency oscillations. One of the most popular implicit integrators is the Hilber-Hughes-Taylor (HHT) method (Hilber et al., 1977). Among the attractive feature

of this method are the stability of the solution and the ability of the method to damp out numerically the small amplitude high frequency oscillations. Negrut et al. (2007) investigated an HHT-based algorithm for Index 3 differential-algebraic equations (DAEs) of multibody systems (HHT-I3), along with strategies for error estimation, integration step size control, and convergence criteria. It is the objective of this paper to examine the use of HHT-I3 in the analysis of flexible bodies modeled using the finite element absolute nodal coordinate formulation by comparing its performance of the HHT-I3 with that of the predictor-corrector explicit Adams integrator (Shampine and Gordon, 1975). It is important, however, to point out that the implicit and explicit integration methods lead to two fundamentally different numerical solution procedures. When the implicit integrator is used, there is no need to use the generalized coordinate partitioning method in order to check on the violation of the kinematic constraints. The fundamental differences between the two solution procedures will be discussed in this paper.

This paper is organized as follows. A brief introduction of the absolute nodal coordinate formulation and the DAEs governing the nonlinear dynamics of multibody systems is provided in Section 2. In Sections 3 - 6, the HHT-I3 method, along with its error estimation, selection of the time step size, and convergence criterion are discussed. In Section 7, the predictor-corrector Adams integration method and the associated numerical procedure used in this study are reviewed. Numerical examples are presented in Section 8 to compare between the performances of the implicit and explicit integrators. In these examples, the flexible structures are modeled using the absolute nodal coordinate formulation. The Adams explicit integrator does not produce numerical damping, while the implicit HHT-I3 method provides adjustable numerical damping. A two-dimensional flexible pendulum example is used in this comparison. The same pendulum example is solved for different values of the modulus of elasticity in order to show the effect of the stiffness on the solution accuracy and integrator efficiency. Summary and main conclusions of this study are presented in Section 9.

2. Constrained Multibody System Equations

In the implicit numerical integration procedure used in this investigation, the equations of motion are presented in the Index 3 augmented form (Brenan et al., 1989). These equations are expressed in terms of the kinematic constraint Jacobian matrix and Lagrange multipliers which can be used to determine the generalized constraint forces. The implicit and explicit methods used in this investigation to solve the resulting dynamics equations lead to two fundamentally different numerical solution procedures. For instance, the explicit method requires the use of the generalized coordinate partitioning, while the implicit method does not require the identification of the system degrees of freedom.

In this study, flexible bodies are modeled using the finite element absolute nodal coordinate formulation. In this formulation, the global position vector $\mathbf{r}$ of an arbitrary point on the finite element j of the flexible body i is defined as

$$\mathbf{r}^{ij} = \mathbf{S}^{ij}\left(\mathbf{x}^{ij}\right)\mathbf{e}^{ij}\left(t\right) \tag{1}$$

where $\mathbf{S}^{ij}$ is the space dependent element shape function, $\mathbf{x}^{ij}$ is the vector of the element spatial coordinates, $\mathbf{e}^{ij}$ is the vector of the time-dependent element nodal coordinates, and t is time. The vector of nodal coordinates contains absolute position and gradient coordinates. Using the principle of virtual work, the finite element equations of motion expressed in terms of the nodal coordinates can be written in the following matrix form (Shabana, 2005):

$$\mathbf{M}^{ij}\ddot{\mathbf{e}}^{ij} = \mathbf{Q}_k^{ij} + \mathbf{Q}_e^{ij} \tag{2}$$

where $\mathbf{Q}_k^{ij}$ is the vector of generalized element elastic forces, $\mathbf{Q}_e^{ij}$ is the vector of generalized element external forces, and $\mathbf{M}^{ij}$ is the element constant symmetric mass matrix which is defined by the following equation:

$$\mathbf{M}^{ij} = \int_{V^{ij}} \rho^{ij} \mathbf{S}^{ij\mathrm{T}} \mathbf{S}^{ij} dV^{ij} \tag{3}$$

In this equation ρ^{ij} and V^{ij} are the element mass density and volume. While the mass matrix is constant, the vector of the elastic forces in the absolute nodal coordinate formulation is a highly nonlinear function of the nodal coordinates. Several methods based on different models can be used to evaluate the elastic forces (Schwab and Meijaard, 2005; Hussein et al., 2007). If a general continuum mechanics approach is used to formulate the elastic forces, one obtains a model that includes the ANCF coupled deformation modes. On the other hand, if an elastic line approach is used, the ANCF coupled deformation modes can be systematically eliminated. In this investigation, the general continuum mechanics approach is used to formulate the elastic forces.

Using the finite element equations, the equations of motion of the multibody system subject to kinematic constraints can be written in the following form:

$$\left.\begin{aligned} \mathbf{M}\ddot{\mathbf{q}} + \mathbf{C}_\mathbf{q}^{\mathrm{T}}\boldsymbol{\lambda} &= \mathbf{Q} \\ \mathbf{C}(\mathbf{q}, t) &= \mathbf{0} \end{aligned}\right\} \tag{4}$$

In this equation, $\mathbf{M}$ is the system mass matrix, $\mathbf{q}$ is the vector of the system coordinates including the absolute nodal coordinates and other coordinates used to describe the motion of rigid bodies, $\boldsymbol{\lambda}$ is the vector of Lagrange multipliers, $\mathbf{Q}$ is the vector of all forces including external, elastic, Coriolis and centrifugal forces, $\mathbf{C}$ is the vector of the constraint functions, and $\mathbf{C}_\mathbf{q}$ is the Jacobian matrix of the kinematic constraint equations.

The HHT-I3 implicit and the Adams explicit methods used in this investigation to solve the constrained system of Eq. 4 lead to two fundamentally different numerical procedures. In the explicit method, the generalized coordinate partitioning is used, and the constraint equations are imposed at the position, velocity and acceleration levels. The dynamic equations and the constraint equations at the acceleration levels are solved for the system accelerations and Lagrange multipliers. The independent accelerations are identified and integrated forward in time in order to determine the dependent coordinates and velocities. Dependent variables are determined using the constraint equations at the position and velocity levels. At the position level, an iterative Newton-Raphson procedure is used to determine the dependent coordinates. The implicit method, on the other hand, does not require the identification of the independent coordinates (degrees of freedom), and the constraint equations are imposed at the position level only. The extension of this implicit procedure to satisfy the kinematic constraints at the velocity

level, when the absolute nodal coordinate formulation is used, will be addressed in future investigations.

3. Background

The HHT-I3 method used in this investigation is based on the Hilber-Hughes-Taylor method (also known to as the α-method) (Hilber et al., 1977). This method is widely used in solving numerically second order initial value problems in structural dynamics. The foundation of the HHT method is the Newmark method which was proposed by Newmark (1959). For this reason, the Newmark method is briefly reviewed in this section in order to have an understanding of the implicit procedure used and the inherent numerical damping that characterizes the HTT method that will be discussed in subsequent sections.

The Newmark method provides a solution for the structural dynamics equations of motion which has the following standard form:

$$\mathbf{M}\ddot{\mathbf{q}} + \mathbf{C}\dot{\mathbf{q}} + \mathbf{K}\mathbf{q} = \mathbf{F}(t) \tag{5}$$

where $\mathbf{q}$, $\dot{\mathbf{q}}$ and $\ddot{\mathbf{q}}$ are the vectors of generalized position coordinates, velocities and accelerations, respectively, $\mathbf{M}$, $\mathbf{C}$ and $\mathbf{K}$ are the symmetric mass, damping and stiffness matrices, respectively, and $\mathbf{F}$ is a time dependent external force vector. Newmark method introduces two equations that relate the position and the velocity vectors to the acceleration vector based on Taylor series expansion. The position vector $\mathbf{q}_{n+1}$ and velocity vector $\dot{\mathbf{q}}_{n+1}$ can be written at time t_{n+1} by using a Taylor series expansion as follows.

$$\mathbf{q}_{n+1} = \mathbf{q}_n + h\dot{\mathbf{q}}_n + \frac{h^2}{2}\ddot{\mathbf{q}}_n + \beta h^3 \dddot{\mathbf{q}}_m \tag{6}$$

$$\dot{\mathbf{q}}_{n+1} = \dot{\mathbf{q}}_n + h\ddot{\mathbf{q}}_n + \gamma h^2 \dddot{\mathbf{q}}_m \tag{7}$$

where $h = t_{n+1} - t_n$ is the step size, m refers to a state somewhere between the states n and $n+1$, and β and γ are two assumed parameters. One can approximate $\dddot{\mathbf{q}}_m$ by using the following equation:

$$\dddot{\mathbf{q}}_m = (\ddot{\mathbf{q}}_{n+1} - \ddot{\mathbf{q}}_n)/h \tag{8}$$

Substituting Eq. 8 into Eqs. 6 and 7 leads to

$$\mathbf{q}_{n+1} = \mathbf{q}_n + h\dot{\mathbf{q}}_n + \frac{h^2}{2}\left((1-2\beta)\ddot{\mathbf{q}}_n + 2\beta\ddot{\mathbf{q}}_{n+1}\right) \tag{9}$$

$$\dot{\mathbf{q}}_{n+1} = \dot{\mathbf{q}}_n + h\left((1-\gamma)\ddot{\mathbf{q}}_n + \gamma\ddot{\mathbf{q}}_{n+1}\right) \tag{10}$$

Equations 9 and Eq. 10 are the Newmark equations that define $\mathbf{q}_{n+1}$ and $\dot{\mathbf{q}}_{n+1}$ as functions of $\mathbf{q}_n$, $\dot{\mathbf{q}}_n$, $\ddot{\mathbf{q}}_n$ and $\ddot{\mathbf{q}}_{n+1}$. By assuming that Eq. 5 is satisfied at any time, one can write the equations of motion at time t_{n+1} as follows:

$$\mathbf{M}\ddot{\mathbf{q}}_{n+1} + \mathbf{C}\dot{\mathbf{q}}_{n+1} + \mathbf{K}\mathbf{q}_{n+1} = \mathbf{F}(t_{n+1}) \tag{11}$$

Substituting Eqs. 9 and 10 into Eq. 11 and assuming that $\mathbf{q}_n$, $\dot{\mathbf{q}}_n$ and $\ddot{\mathbf{q}}_n$ are known, one obtains a set of equations that are functions of the acceleration vector $\ddot{\mathbf{q}}_{n+1}$. Therefore,

these equations can be used to determine the vector of accelerations $\ddot{\mathbf{q}}_{n+1}$, which can be used in turn to determine $\mathbf{q}_{n+1}$ and $\dot{\mathbf{q}}_{n+1}$ using Eqs. 9 and 10.

The stability of the solution obtained using the Newmark method depends on the choice of values for the two parameters γ and β. In order to have a stable solution these parameters should satisfy the following relations (Hilber et al., 1977).

$$\gamma \geq \tfrac{1}{2}\ , \qquad \beta \geq \frac{\left(\gamma+\tfrac{1}{2}\right)^2}{4} \tag{12}$$

If $\gamma = \tfrac{1}{2}$ and $\beta = \tfrac{1}{4}$, one obtains the well known trapezoidal method, which is A-stable and has second order convergence property. The main drawback of the trapezoidal method is that it is not capable of eliminating spurious high frequencies.

The HHT method is an improvement over the Newmark method in that it has the ability to eliminate undesirable high frequency oscillations, while it remains stable and second order convergent. The HHT method can be obtained by replacing Eq. 11 by

$$\mathbf{M}\ddot{\mathbf{q}}_{n+1} + (1+\alpha)\mathbf{C}\dot{\mathbf{q}}_{n+1} - \alpha\mathbf{C}\dot{\mathbf{q}}_n + (1+\alpha)\mathbf{K}\mathbf{q}_{n+1} - \alpha\mathbf{K}\mathbf{q}_n = \mathbf{F}(\tau_{n+1}) \tag{13}$$

where α is an assumed parameter, and

$$\tau_{n+1} = t_n + (1+\alpha)h \tag{14}$$

In order to obtain a stable solution using the implicit HHT method, the parameters α, γ and β should be selected to satisfy the following relations:

$$-0.3 \leq \alpha \leq 0 \qquad \gamma = \tfrac{1}{2} - \alpha \qquad \beta = (1-\alpha)^2/4 \tag{15}$$

The smaller the value of α, the more numerical damping is added to the system. The choice $\alpha = 0$ leads to the trapezoidal method, which has no numerical damping.

4. HHT-I3 method and Multibody Equations

The implicit HHT-I3 uses the HHT method to transform the differential equations of motion of the multibody system into a set of nonlinear algebraic equations. These nonlinear algebraic equations can be solved simultaneously with the nonlinear constraint equations at the position level to determine the state of the system. The differential equations of motion and the constraint equations can be written in the form of Eq. 4, which is reproduced here for convenience

$$\mathbf{M}(\mathbf{q})\ddot{\mathbf{q}} + \mathbf{C}_\mathbf{q}^{\mathrm{T}}\boldsymbol{\lambda} = \mathbf{Q}(t, \mathbf{q}, \dot{\mathbf{q}}) \tag{16}$$

$$\mathbf{C}(\mathbf{q}, t) = \mathbf{0} \tag{17}$$

Note that Eq. 16 can be written as

$$\mathbf{M}\ddot{\mathbf{q}} = \mathbf{H}, \tag{18}$$

where $\mathbf{H} = \mathbf{Q} - \mathbf{C}_\mathbf{q}^{\mathrm{T}}\boldsymbol{\lambda}$ represents the generalized forces including the constraint forces. Recall that when the absolute nodal coordinate formulation is used, the mass matrix is constant. Furthermore, if Cholesky coordinates are used, the mass matrix becomes the identity matrix. This important feature of the finite element absolute nodal coordinate formulation will be exploited when developing an estimate of the local integration error, as discussed in the following section.

Using Eq. 13 which is the formula for the HHT method, Eq. 18 at time step t_{n+1} can be written as

$$\left(\mathbf{M}\ddot{\mathbf{q}}\right)_{n+1} = \mathbf{H}\left(\tau_{n+1}\right). \tag{19}$$

where τ_{n+1} is defined in by Eq. 14. One can use a Taylor series expansion to write

$$\mathbf{H}\left(\tau_{n+1}\right) = \mathbf{H}\left(t_n\right) + \left(1+\alpha\right) h\dot{\mathbf{H}}\left(t_m\right), \tag{20}$$

where t_m is a time between t_n and τ_{n+1}, and $\dot{\mathbf{H}}(t_m)$ can be approximated by assuming liner change in $\mathbf{H}$, that is

$$\dot{\mathbf{H}}(t_m) = \left(\mathbf{H}(t_{n+1}) - \mathbf{H}(t_n)\right)/h\,. \tag{21}$$

By substituting this equation into Eq. 20, and then using the resulting expression of $\dot{\mathbf{H}}\left(\tau_{n+1}\right)$ in Eq. 19, one obtains

$$\left(\mathbf{M}\ddot{\mathbf{q}}\right)_{n+1} = \left(1+\alpha\right)\mathbf{H}(t_{n+1}) - \alpha\mathbf{H}(t_n)\,. \tag{22}$$

Since $\mathbf{H} = \mathbf{Q} - \mathbf{C}_{\mathbf{q}}^{\mathrm{T}}\boldsymbol{\lambda}$, one can write Eq. 22 in the following form:

$$\left(\mathbf{M}\ddot{\mathbf{q}}\right)_{n+1} + \left(1+\alpha\right)\left(\mathbf{C}_{\mathbf{q}}^{\mathrm{T}}\boldsymbol{\lambda} - \mathbf{Q}\right)_{n+1} - \alpha\left(\mathbf{C}_{\mathbf{q}}^{\mathrm{T}}\boldsymbol{\lambda} - \mathbf{Q}\right)_n = \mathbf{0} \tag{23}$$

At time t_{n+1}, the constraints are assumed to be satisfied. Therefore, one can use Eq. 17 to write

$$\mathbf{C}\left(\mathbf{q}_{n+1}, t_{n+1}\right) = \mathbf{0} \tag{24}$$

While Eqs. 23 and 24 depend on $\mathbf{q}_{n+1}$, $\dot{\mathbf{q}}_{n+1}$, $\ddot{\mathbf{q}}_{n+1}$ and $\boldsymbol{\lambda}_{n+1}$, one can use Eqs. 9 and 10 to write these equations (Eqs. 23 and 24) as functions of $\ddot{\mathbf{q}}_{n+1}$ and $\boldsymbol{\lambda}_{n+1}$ only. The result is a set of nonlinear algebraic equations that can be solved for $\ddot{\mathbf{q}}_{n+1}$ and $\boldsymbol{\lambda}_{n+1}$ using an iterative Newton-Raphson method. The iterative Newton-Raphson method requires constructing and solving the following system of equations at iteration k:

$$\begin{bmatrix} \dfrac{\partial \mathbf{F}_1}{\partial \ddot{\mathbf{q}}_{n+1}} & \dfrac{\partial \mathbf{F}_1}{\partial \boldsymbol{\lambda}_{n+1}} \\ \dfrac{\partial \mathbf{F}_2}{\partial \ddot{\mathbf{q}}_{n+1}} & \dfrac{\partial \mathbf{F}_2}{\partial \boldsymbol{\lambda}_{n+1}} \end{bmatrix}^{(k)} \begin{bmatrix} \Delta\ddot{\mathbf{q}}_{n+1} \\ \Delta\boldsymbol{\lambda}_{n+1} \end{bmatrix}^{(k)} = -\begin{bmatrix} \mathbf{F}_1 \\ \mathbf{F}_2 \end{bmatrix}^{(k)}, \tag{25}$$

where Δ indicates Newton differences, and $\mathbf{F}_1$ and $\mathbf{F}_2$ are defined as

$$\left.\begin{aligned} \mathbf{F}_1 &= \frac{1}{1+\alpha}\left(\mathbf{M}\ddot{\mathbf{q}}\right)_{n+1} + \left(\mathbf{C}_{\mathbf{q}}^{\mathrm{T}}\boldsymbol{\lambda} - \mathbf{Q}\right)_{n+1} - \frac{\alpha}{1+\alpha}\left(\mathbf{C}_{\mathbf{q}}^{\mathrm{T}}\boldsymbol{\lambda} - \mathbf{Q}\right)_n \\ \mathbf{F}_2 &= \frac{1}{\beta h^2}\mathbf{C}\left(\mathbf{q}_{n+1}, t_{n+1}\right) \end{aligned}\right\} \tag{26}$$

Using these vector functions, one can show that, instead of using numerical differentiation, $\left(\partial\mathbf{F}_1/\partial\boldsymbol{\lambda}_{n+1}\right)$, $\left(\partial\mathbf{F}_2/\partial\boldsymbol{\lambda}_{n+1}\right)$ and $\left(\partial\mathbf{F}_2/\partial\ddot{\mathbf{q}}_{n+1}\right)$ can be obtained in analytical form from the following equations:

$$\left.\begin{aligned} \frac{\partial \mathbf{F}_1}{\partial \boldsymbol{\lambda}_{n+1}} &= \mathbf{C}_{\mathbf{q}}^{\mathrm{T}}, \qquad \frac{\partial \mathbf{F}_2}{\partial \boldsymbol{\lambda}_{n+1}} = \mathbf{0} \\ \frac{\partial \mathbf{F}_2}{\partial \ddot{\mathbf{q}}_{n+1}} &= \frac{1}{\beta h^2}\frac{\partial \mathbf{C}}{\partial \mathbf{q}_{n+1}}\frac{\partial \mathbf{q}_{n+1}}{\partial \ddot{\mathbf{q}}_{n+1}} = \mathbf{C}_{\mathbf{q}} \end{aligned}\right\} \tag{27}$$

The value of $\partial \mathbf{F}_1 / \partial \ddot{\mathbf{q}}_{n+1}$, however, is calculated by numerical differentiation.

Since constructing the Jacobian of Eq. 25 is expensive, it is recommended against updating this Jacobian at each Newton iteration. In order to avoid a bad condition number of the coefficient matrix in Eq. 25 when $h \to 0$, Eq. 24 was divided by βh^2 to obtain the second equation of Eq. 26. The interested reader is referred to Negrut et al. (2007) for a more complete discussion of this topic.

5. Integration Error and Time Step

In order to have a measure of the accuracy of the obtained solution, one must have an accurate estimate of the local integration error. In this section, a procedure for the error estimation is discussed. Since the mass matrix, in general, depends on the coordinates only, it can be assumed, in many applications, that the change in the mass matrix with respect to time is small over a certain period of time. In fact, in the case of the absolute nodal coordinate formulation, the mass matrix remains constant, and if Cholesky coordinates are used this mass matrix becomes the identity matrix, as previously discussed. In this case, one can write the derivative of Eq. 18 with respect to time at t_n as follows.

$$\mathbf{M}\dddot{\mathbf{q}}_n = \dot{\mathbf{H}}(t_n) \tag{28}$$

An equation similar to Eq. 21 can be used to approximate the value of $\dot{\mathbf{H}}(t_n)$. This leads to

$$\mathbf{M}\dddot{\mathbf{q}}_n = (\mathbf{H}(t_{n+1}) - \mathbf{H}(t_n))/h\,. \tag{29}$$

Assuming that the equations of motion are satisfied at t_n , one has

$$\mathbf{M}\ddot{\mathbf{q}}_n = \mathbf{H}(t_n)\,, \tag{30}$$

Subtracting this equation from Eq. 22 and using Eq. 29, one obtains

$$\ddot{\mathbf{q}}_{n+1} - \ddot{\mathbf{q}}_n = h(1+\alpha)\dddot{\mathbf{q}}_n \tag{31}$$

A Taylor series expansion of the exact solution $(\mathbf{q}_{n+1})_e$ of the equation of motion at t_{n+1} is given by

$$(\mathbf{q}_{n+1})_e = \mathbf{q}_n + h\dot{\mathbf{q}}_n + \frac{h^2}{2}\ddot{\mathbf{q}}_n + \frac{h^3}{6}\dddot{\mathbf{q}}_n + O\left(h^4\right) \tag{32}$$

An estimate of the local integration error $\boldsymbol{\delta}_{n+1}$ can be computed by subtracting the exact solution from the solution obtained using the numerical integration. This estimate is given by

$$\boldsymbol{\delta}_{n+1} = \mathbf{q}_{n+1} - (\mathbf{q}_{n+1})_e \tag{33}$$

Substituting the values of $\mathbf{q}_{n+1}$ and $(\mathbf{q}_{n+1})_e$ from Eq. 9 and Eq. 32, respectively, into Eq. 33 yields

$$\boldsymbol{\delta}_{n+1} = \beta h^2 (\ddot{\mathbf{q}}_{n+1} - \ddot{\mathbf{q}}_n) - \frac{h^3}{6} \dddot{\mathbf{q}}_n - O(h^4) \tag{34}$$

By substituting the value of $\dddot{\mathbf{q}}_n$ from Eq. 31 and neglecting higher order terms, one obtains

$$\boldsymbol{\delta}_{n+1} \approx \left(\beta - \frac{1}{6(1+\alpha)} \right) h^2 (\ddot{\mathbf{q}}_{n+1} - \ddot{\mathbf{q}}_n) \tag{35}$$

In order to accept the obtained solution, a norm of the error function must be less than a user specified tolerance. The following weighted norm for the vector of the local integration error was proposed by Negrut et al. (2007):

$$e = \sqrt{\frac{1}{p} \sum_{i=1}^{p} \left(\frac{\delta_{i,n+1}}{Y_i} \right)^2} \tag{36}$$

where $Y_i = \max\left(1, \max_{j=1,\ldots,n} |q_{i,j}|\right)$ is the i^{th} component of the weighting vector $\mathbf{Y}_i$, and p is the number of elements of the position coordinate vector $\mathbf{q}$. The error function of Eq. 36 can be written as

$$e = \left| \beta - \frac{1}{6(1+\alpha)} \right| \frac{h^2}{\sqrt{p}} \|\mathbf{x}\| \tag{37}$$

where $\mathbf{x} = (\ddot{\mathbf{q}}_{n+1} - \ddot{\mathbf{q}}_n)$, and $\|\cdot\|$ represents the weighted norm, that is $\|\mathbf{x}\| = \sqrt{\sum_{i=1}^{p} \left(\frac{x_i}{Y_i} \right)^2}$.

The error must be less than the user specified tolerance ε, that is, $e \le \varepsilon$. This is equivalent to

$$\Theta \le 1 \tag{38}$$

where Θ is defined as

$$\Theta = \frac{\|\mathbf{x}\|^2 h^4}{\psi} \tag{39}$$

and

$$\psi = \frac{p \varepsilon^2}{\left(\beta - \frac{1}{6(1+\alpha)} \right)^2} \tag{40}$$

The step-size selection is an important issue in developing efficient numerical integration methods. A very small step-size may lead to additional unnecessary calculations for the desired accuracy. On the other hand, a very large step-size may lead to an increase in the number of Newton-Raphson iterations required to achieve convergence. Furthermore, a large step size may result in a numerical solution that is not accurate enough. The step-size should be selected to accelerate the convergence in the next time step with an integration error within the limit specified by the user. In order to

describe the procedure used in this investigation to select the step size, the definition $\mathbf{x} = \left(\ddot{\mathbf{q}}_{n+1} - \ddot{\mathbf{q}}_n\right)$ and Eq. 31 are used to write $\mathbf{x}$ as a function of $\ddot{\mathbf{q}}_n$ as follows:

$$\mathbf{x} = h\left(1+\alpha\right)\dddot{\mathbf{q}}_n \tag{41}$$

By assuming that there is no significant change in $\ddot{\mathbf{q}}_n$ and weighting vector $\mathbf{Y}_i$ between two consecutive time steps, one can define a constant a as follows:

$$a = \left(1+\alpha\right)^2\left(\sum_{i=1}^{p}\left(\frac{\dddot{q}_{i,n}}{Y_i}\right)^2\right) \tag{42}$$

By using the preceding two equations and the definition of the norm $\|\cdot\|$, one obtains

$$\|\mathbf{x}\|^2 = ah^2 \tag{43}$$

By substituting $\|\mathbf{x}\|^2$ from this equation into Eq. 39, one obtains

$$\Theta = \frac{ah^6}{\psi} \tag{44}$$

The new step-size h_{new} should be selected such that the integration error is within the user specified tolerance, or equivalently, $\Theta_{new} = 1$. Therefore,

$$\frac{ah_{new}^6}{\psi} = 1 \tag{45}$$

In this investigation, a safety factor $s = 0.9$ is introduced. The preceding two equations can then be used to obtain an estimate of the new step-size as follows:

$$h_{new} = \frac{sh}{\Theta^{\frac{1}{6}}} \tag{46}$$

This equation is used in this study to determine the new step-size.

6. Convergence Criterion

Having developed a procedure for error estimation and step size selection, one needs to establish a criterion for stopping the iteration process. This criterion determines how accurately Eq. 23 should be satisfied, or in other words, how accurately should the vector $\ddot{\mathbf{q}}_{n+1}$ be calculated before the result are accepted by the user. In order to develop the convergence criterion, assume that the exact value of the vector $\ddot{\mathbf{q}}_{n+1}$ is approximated after k iterations by $\ddot{\mathbf{q}}_{n+1}^{(k)}$. In this case, one can write the local error after k iterations by using Eq. 37 as follows:

$$e^{(k)} = \left|\beta - \frac{1}{6\left(1+\alpha\right)}\right|\frac{h^2}{\sqrt{p}}\left\|\mathbf{x}^{(k)}\right\| \tag{47}$$

where $\left\|\mathbf{x}^{(k)}\right\|$ is the approximated value of $\|\mathbf{x}\|$, that is, $\mathbf{x}^{(k)} = \left(\ddot{\mathbf{q}}_{n+1}^{(k)} - \ddot{\mathbf{q}}_n\right)$.

Convergence is assumed if the relative error between e and $e^{(k)}$ is less than a certain specified value c, that is, $\left|\left(e - e^{(k)}\right)/e\right| \le c$. Since the value of e is not available, it

is approximated in the denominator by ε, and the convergence test can be written as follows:

$$\left|\frac{e-e^{(k)}}{\varepsilon}\right| \le c \tag{48}$$

By using Eq. 37 and Eq. 47, one can write

$$\left|e-e^{(k)}\right| \le \left|\beta - \frac{1}{6(1+\alpha)}\right| \frac{h^2}{\sqrt{p}} \left\|\mathbf{x}-\mathbf{x}^{(k)}\right\| \tag{49}$$

In order to obtain an approximation for $\left\|\mathbf{x}-\mathbf{x}^{(k)}\right\|$, one can use the linear convergence property of Newton method, which assumes that there is a constant ξ, $0 \le \xi < 1$, such that

$$\left\|\Delta\mathbf{x}^{(k+1)}\right\| \le \xi \left\|\Delta\mathbf{x}^{(k)}\right\| \tag{50}$$

where $\Delta\mathbf{x}^{(k)}$ is the correction at the iteration k, $\Delta\mathbf{x}^{(k)} = \mathbf{x}^{(k)} - \mathbf{x}^{(k-1)}$. The inequality of Eq. 50 can be used to write the following:

$$\left\|\Delta\mathbf{x}^{(k+n)}\right\| \le \xi^n \left\|\Delta\mathbf{x}^{(k)}\right\| \tag{51}$$

Since $\mathbf{x}^{(k+m)} - \mathbf{x}^{(k)} = \left(\mathbf{x}^{(k+m)} - \mathbf{x}^{(k+m-1)}\right) + \mathbf{x}^{(k+m-1)} + \ldots\ldots - \mathbf{x}^{(k+1)} + \left(\mathbf{x}^{(k+1)} - \mathbf{x}^{(k)}\right) = \sum_{i=1}^{m} \Delta\mathbf{x}^{(k+i)}$,

one can write

$$\left\|\mathbf{x}^{(k+m)} - \mathbf{x}^{(k)}\right\| \le \sum_{i=1}^{m} \left\|\Delta\mathbf{x}^{(k+i)}\right\| \tag{52}$$

Using the inequalities of Eqs. 51 and 52, one can write

$$\left\|\mathbf{x}^{(k+m)} - \mathbf{x}^{(k)}\right\| \le \left\|\Delta\mathbf{x}^{(k)}\right\| \sum_{i=1}^{m} \xi^i \tag{53}$$

Assuming that $\mathbf{x}^{(k)}$ converges to $\mathbf{x}$ after a large number of iterations, that is, $\mathbf{x} = \lim_{m\to\infty} \mathbf{x}^{(k+m)}$, and since for $0 \le \xi < 1$, $\sum_{i=1}^{\infty} \xi^i = \frac{\xi}{1-\xi}$, then

$$\left\|\mathbf{x}-\mathbf{x}^{(k)}\right\| \le \left\|\Delta\mathbf{x}^{(k)}\right\| \frac{\xi}{1-\xi} \tag{54}$$

Using the inequalities of Eqs. 49 and 54, one has

$$\left|e-e^{(k)}\right| \le \left|\beta - \frac{1}{6(1+\alpha)}\right| \frac{h^2}{\sqrt{p}} \left\|\Delta\mathbf{x}^{(k)}\right\| \frac{\xi}{1-\xi} \tag{55}$$

From Eqs. 40 and 55, the convergence test of Eq. 48 is satisfied if the following condition is met:

$$\left(\frac{\xi}{1-\xi}\right)^2 \left\|\Delta\mathbf{x}^{(k)}\right\|^2 \le c^2 \frac{\psi}{h^4} \tag{56}$$

This is the convergence test used in the HHT-I3 method employed in this investigation that is focused on the absolute nodal coordinate formulation models.

In summary, the procedure used in the implicit HHT-I3 method described in this study requires an initial guess of $\ddot{\mathbf{q}}_{n+1}$ and $\boldsymbol{\lambda}_{n+1}$ which can be made using Newton differences or values obtained at the previous time step. Equation 25 is then solved

iteratively to find more accurate solution for $\ddot{\mathbf{q}}_{n+1}$ and $\boldsymbol{\lambda}_{n+1}$. After at least two iterations, the parameter ξ can be calculated, and the convergence condition of Eq. 56 is tested. If this condition is not satisfied, then more iterations are required. If the condition is satisfied, then the condition of Eq. 38 is tested. If this condition is satisfied, then the new step-size is updated using Eq. 46, and the integrator proceeds to the next time step. If the condition of Eq. 38 is not satisfied, then the step-size has to be updated using Eq. 46 and the same time step solution has to be reevaluated.

7. Explicit ADAMS Method

The Adams method is an explicit predictor-corrector method for the numerical solution of first order ordinary differential equations. This method can not be used to directly solve a system of DAEs. The algebraic equations must be first eliminated using the generalized coordinate partitioning technique, which is in principle equivalent to the *embedding technique* (Shabana, 2005). The embedding technique, that eliminates the reaction forces and the dependent coordinates, leads to a minimum set of differential equations expressed in terms of the independent coordinates (degrees of freedom) only. Using the generalized coordinate partitioning, one can write the system coordinates as follows:

$$\mathbf{q} = \begin{bmatrix} \mathbf{q}_i^{\mathrm{T}} & \mathbf{q}_d^{\mathrm{T}} \end{bmatrix}^{\mathrm{T}} \tag{57}$$

where $\mathbf{q}_i$ is the vector of independent coordinates or degrees of freedom, and $\mathbf{q}_d$ is the vector of dependent coordinates. One can define the velocity transformation matrix $\mathbf{B}_{di}$ that relates the system velocities to the independent velocities ($\dot{\mathbf{q}} = \mathbf{B}_{di}\dot{\mathbf{q}}_i$) as follows.

$$\mathbf{B}_{di} = \begin{bmatrix} \mathbf{I} \\ -\mathbf{C}_{\mathbf{q}_d}^{-1}\mathbf{C}_{\mathbf{q}_i} \end{bmatrix} \tag{58}$$

By pre-multiplying Eq. 16 by $\mathbf{B}_{di}^{\mathrm{T}}$, one obtains

$$\mathbf{B}_{di}^{\mathrm{T}}\mathbf{M}\ddot{\mathbf{q}} + \mathbf{B}_{di}^{\mathrm{T}}\mathbf{C}_{\mathbf{q}}^{\mathrm{T}}\boldsymbol{\lambda} = \mathbf{B}_{di}^{\mathrm{T}}\mathbf{Q} \tag{59}$$

It can be shown that (Shabana, 2005)

$$\mathbf{B}_{di}^{\mathrm{T}}\mathbf{C}_{\mathbf{q}}^{\mathrm{T}} = \mathbf{0} \tag{60}$$

By taking the second derivative of the nonlinear algebraic constraint equations of Eq. 17 with respect to time, one obtains

$$\mathbf{C}_{\mathbf{q}}\ddot{\mathbf{q}} = \mathbf{Q}_d \tag{61}$$

where $\mathbf{Q}_d = -\mathbf{C}_{tt} - 2\mathbf{C}_{\mathbf{q}t} - \left(\mathbf{C}_{\mathbf{q}}\dot{\mathbf{q}}\right)_{\mathbf{q}}\dot{\mathbf{q}}$ is a vector that is quadratic in the velocities. One can rewrite Eq. 61 in terms of $\mathbf{q}_i$ and $\mathbf{q}_d$ as follows:

$$\mathbf{C}_{\mathbf{q}_i}\ddot{\mathbf{q}}_i + \mathbf{C}_{\mathbf{q}_d}\ddot{\mathbf{q}}_d = \mathbf{Q}_d \tag{62}$$

Using Eqs. 57, 58 and 62, one has

$$\ddot{\mathbf{q}} = \mathbf{B}_{di}\ddot{\mathbf{q}}_i + \bar{\mathbf{Q}}_d \tag{63}$$

where $\bar{\mathbf{Q}}_d = \begin{bmatrix} \mathbf{0} & \left(\mathbf{C}_{\mathbf{q}_d}^{-1}\mathbf{Q}_d\right)^{\mathrm{T}} \end{bmatrix}^{\mathrm{T}}$. Substituting Eq. 63 into Eq. 59 and using Eq. 60 yields

$$\mathbf{B}_{di}^{\mathrm{T}}\mathbf{M}\mathbf{B}_{di}\ddot{\mathbf{q}}_i + \mathbf{B}_{di}^{\mathrm{T}}\mathbf{M}\bar{\mathbf{Q}}_d = \mathbf{B}_{di}^{\mathrm{T}}\mathbf{Q} \tag{64}$$

This system of equations is expressed in terms of the independent coordinates, leading to the elimination of the constraint forces.

In order to use the explicit Adams method, one has to transform the second order differential equations into a system of first order ordinary differential equations (ODEs). This is accomplished by introducing a new vector $\mathbf{y}$, defined as

$$\mathbf{y} = \begin{bmatrix} \mathbf{q}_i^{\mathrm{T}} & \dot{\mathbf{q}}_i^{\mathrm{T}} \end{bmatrix}^{\mathrm{T}} \tag{65}$$

Taking the time derivative of this vector and substituting the value of $\ddot{\mathbf{q}}_i$ from the solution of Eq. 64 yields

$$\dot{\mathbf{y}} = \begin{bmatrix} \dot{\mathbf{q}}_i \\ \left(\mathbf{B}_{di}^{\mathrm{T}}\mathbf{M}\mathbf{B}_{di}\right)^{-1}\left(\mathbf{B}_{di}^{\mathrm{T}}\mathbf{Q} - \mathbf{B}_{di}^{\mathrm{T}}\mathbf{M}\bar{\mathbf{Q}}_d\right) \end{bmatrix} \tag{66}$$

Note that the right hand side of this equation is a function of $\mathbf{q}_i$, $\dot{\mathbf{q}}_i$ and t. Therefore, the original problem is reformulated as

$$\dot{\mathbf{y}} = \mathbf{f}(\mathbf{y}, t), \tag{67}$$

which is the standard form of a first order ODE that can be solved using the Adams method. The explicit Adams method used in this study is the *Adams-Predictor-Corrector* method discussed by Shampine and Gordon (1975). In this method, a predicted value $\mathbf{y}_{n+1}^{p}$ at time step t_{n+1} based on the solution at time step t_n and several previous values of $\mathbf{f}$ is obtained by using the Adams-Bashforth formula:

$$\mathbf{y}_{n+1}^{p} = \mathbf{y}_n + \int_{t_n}^{t_{n+1}} \mathbf{P}_{m,n}(t)\ dt\,. \tag{68}$$

Here $\mathbf{P}_{m,n}(t)$ is a Lagrange interpolating polynomial that interpolates the previous m values of $\mathbf{f}(\mathbf{y}, t)$, that is,

$$\mathbf{P}_{m,n}(t) = \sum_{j=1}^{m} \mathbf{f}_{n+1-j} \left(\prod_{\substack{k=1 \\ k \neq j}}^{m} \frac{t - t_{n+1-k}}{t_{n+1-j} - t_{n+1-k}} \right) \tag{69}$$

With $\mathbf{y}_{n+1}^{p}$ available, one can then find the value of $\mathbf{f}_{n+1}^{p}\left(\mathbf{y}_{n+1}^{p}, t_{n+1}\right)$. The corrector Adams-Moulton formula is then used to find a corrected value of $\mathbf{y}_{n+1}^{p}$, which is denoted by $\mathbf{y}_{n+1}$:

$$\mathbf{y}_{n+1} = \mathbf{y}_n + \int_{t_n}^{t_{n+1}} \mathbf{P}_{m,n}^{*}(t)\,dt\,. \tag{70}$$

Here $\mathbf{P}_{m,n}^{*}(t)$ is an interpolating polynomial that interpolates the previous m points in addition to the predicted value $\mathbf{f}_{n+1}^{p}$, that is

$$\mathbf{P}_{m,n}^{*}(t) = \mathbf{f}_{n+1}^{p} \left(\prod_{k=1}^{m} \frac{t - t_{n+1-k}}{t_{n+1} - t_{n+1-k}} \right) + \sum_{j=1}^{m} \mathbf{f}_{n+1-j} \left(\prod_{\substack{k=0 \\ k \neq j}}^{m} \frac{t - t_{n+1-k}}{t_{n+1-j} - t_{n+1-k}} \right) \tag{71}$$

One can then use the corrected value $\mathbf{y}_{n+1}$ to evaluate the function $\mathbf{f}_{n+1}$ which is used in the next time step. A full discussion of the procedures used in this explicit method for

error control and selection of the order and time step can be found in the literature (Shampine, and Gordon, 1975).

There are two points that need to be emphasized when the explicit Adams method is used. First, the integration in Eqs. 68 and 70 can be easily performed analytically, and in fact Shampine and Gordon (1975) provide closed form solutions for those integrals. Second, at every time step the number of points used in the interpolation should be less than or equal to n; thus, at the beginning of the simulation, there is no sufficient number of points to start the integration with a higher order formula. For this reason, a lower order formula is used until information at a sufficient number of points becomes available.

The formal derivation of the embedding formulation presented in this section shows that the mass matrix associated with the independent coordinates may not be, in general, a sparse matrix. In the actual implementation of the embedding formulation, full advantage is taken of sparse matrix techniques at the position, velocity and acceleration levels. For example, the constraint equations at the velocity level can be written as

$$\mathbf{C}_{\mathbf{q}}\dot{\mathbf{q}} = -\mathbf{C}_t \tag{72}$$

If the independent velocities are assumed to be known from the numerical integration, an elementary matrix $\mathbf{I}_d$ that has zeros and ones can be easily constructed. This matrix can be used to extract the independent coordinates or velocities from the total vector of the system coordinates or velocities. Therefore, this constant sparse matrix satisfies the following relation:

$$\mathbf{I}_d\mathbf{q} = \mathbf{q}_i \,. \tag{73}$$

By combining the preceding two equations, one has (Shabana, 2001)

$$\begin{bmatrix} \mathbf{C}_{\mathbf{q}} \\ \mathbf{I}_d \end{bmatrix}\dot{\mathbf{q}} = \begin{bmatrix} -\mathbf{C}_t \\ \dot{\mathbf{q}}_i \end{bmatrix} \tag{74}$$

The solution of this system of algebraic equations defines the dependent coordinates. Note that the coefficient matrix in this equation is also sparse, and therefore, efficient sparse matrix techniques can be used. A similar procedure can be used at the position level when the iterative Newton-Raphson method is used to solve the nonlinear algebraic constraint equations for the dependent coordinates. This can be achieved by replacing in the preceding equation $\dot{\mathbf{q}}$, $\dot{\mathbf{q}}_i$ and $\mathbf{C}_t$ by $\Delta\mathbf{q}$, $\mathbf{0}$ and $\mathbf{C}$, respectively. Similarly, the total vector of accelerations can be determined by solving the augmented form of the equations of motion obtained by combining the first equation in Eq. 16 with Eq. 61, leading to

$$\begin{bmatrix} \mathbf{M} & \mathbf{C}_{\mathbf{q}}^{\mathrm{T}} \\ \mathbf{C}_{\mathbf{q}} & \mathbf{0} \end{bmatrix}\begin{bmatrix} \ddot{\mathbf{q}} \\ \boldsymbol{\lambda} \end{bmatrix} = \begin{bmatrix} \mathbf{Q} \\ \mathbf{Q}_d \end{bmatrix} \tag{75}$$

The coefficient matrix in this equation is again a sparse matrix. Therefore, by using sparse matrix techniques, the preceding equation can be solved efficiently for the accelerations and Lagrange multipliers. The independent accelerations can be identified and integrated forward in time using the explicit integration method. Therefore, in the actual implementation of the embedding technique, full advantage is taken of sparse matrix techniques. Furthermore, there is no need to identify the constraint subjacobian matrices $\mathbf{C}_{\mathbf{q}_i}$ and $\mathbf{C}_{\mathbf{q}_d}$ or find the inverse of $\mathbf{C}_{\mathbf{q}_d}$.

8. Numerical Examples

In order to compare the performance of the implicit HHT-I3 and the explicit Adams methods, a dynamic simulation of a flexible pendulum is performed by using the two integration methods. The pendulum used in this example is assumed to be initially horizontal, as shown in Fig. 1. The pendulum is assumed to fall under the effect of the gravity force. The pendulum model is developed using the finite element absolute nodal coordinate formulation. The beam in this pendulum example is divided into two two-dimensional finite beam elements along its length (Omar and Shabana, 2001). The pendulum beam is assumed to have an undeformed length of 0.4 m, cross sectional area of 0.04×0.04 m^2, a density of 7800 kg/m^3, and a Poisson ratio of 0.3. In order to examine the effect of the stiffness of the beam on the performance of the implicit and explicit integration methods, several values of the beam modulus of elasticity are used. The pendulum example is solved by assuming the following moduli of elasticity: 2×10^5, 2×10^6, 2×10^7, 2×10^8, 2×10^9, 2×10^{10} and 2×10^{11} N/m^2.

The beam elastic forces are formulated using the general continuum mechanics approach. This approach leads to the ANCF coupled deformation modes that also include Poisson modes. For all stiffness levels, these modes couple the deformation of the cross section with bending and extension of the beam. For very stiff structures, the ANCF coupled deformation modes, as previously mentioned, can be associated with very high frequencies. An eigenvalue study of these frequencies was presented in the literature (Schwab and Meijaard, 2005). Explicit integration methods have shown to perform poorly in the presence of these modes in the case of very stiff structures.

Figure 2 shows the vertical position of the pendulum tip when the modulus of elasticity is equal to 2×10^5 N/m^2. The results presented in this figure show the solutions obtained using the two integration methods. Figure 3 shows the mid-point transverse deformation, which is defined as shown in Fig. 4, for the same value of the modulus of elasticity. It is clear from the results presented in these figures that there is no significant difference between the solutions obtained using the two integrators. Figure 5 shows the mid-point transverse deformation when the modulus of elasticity is 2×10^8 N/m^2. The results presented in this figure show that, for this moderate stiffness, the results of the two integrators are almost the same, and that there is still a good agreement between the solutions obtained using the implicit and explicit integration methods. As an example of a highly stiff structure, the simulation was performed assuming a modulus of elasticity of 2×10^{11} N/m^2. Figure 6 shows the vertical position of the pendulum tip for the stiff structure case. The results presented in this figure do not show significant difference between the two reference motion solutions, and therefore, the numerical damping of the HHT-I3 method does not have a significant effect on the rigid body motion of the beam. Figure 7 shows the mid-point transverse deformation for this relatively high modulus of elasticity. It is clear from the results presented in this figure that the implicit HHT-I3 method damped out some high frequency oscillations and it produces a smoother solution than the one obtained by the explicit Adams method.

Figure 8 shows the performance, in terms of CPU time, of the two integrators as function of the modulus of elasticity. The results suggest that there is no significant difference in CPU simulation time between the implicit HHT-I3 method and the explicit Adams method in the case of very flexible structure. As the stiffness of the structure increases with the increase in the modulus of elasticity, the CPU time of the explicit Adams method grows exponentially. In the case of such stiff structures, the implicit HHT-I3 method is much more efficient, and it is capable of damping out the ANCF coupled deformation modes, which for the stiff structure do not have a significant effect on the accuracy of the solution.

9. Summary and Conclusions

Unlike existing finite element structural element formulations, the absolute nodal coordinate formulation allows for the use of the general continuum mechanics theory to formulate the structural element elastic forces. The use of the general continuum mechanics approach to formulate the elastic forces leads to the ANCF coupled deformation modes, including Poisson modes. These modes couple the cross section deformations and bending and extension of the structural elements, as discussed in the literature (Schwab and Meijaard, 2005; Hussein et al., 2007). In the case of very flexible structures, the effect of the ANCF coupled deformation modes can be significant as they capture dynamic effects that can not be captured using existing finite element beam models. In this case of very flexible structures, the ANCF coupled deformation modes are not a source of numerical problems, and explicit integration methods have proven to be efficient. For very stiff structures, on the other hand, the ANCF coupled deformation modes can be associated with very high frequencies. In these special cases, if the deformation shape is simple, instead of the absolute nodal coordinate formulation, it is recommended to use the floating frame of reference formulation, which systematically eliminates high frequency modes. If the deformation shape is complex, such that there is no clear advantage of using the floating frame of reference formulation, the absolute nodal coordinate formulation can still be used with implicit numerical integration methods, as demonstrated in this study.

In order to examine the performance of the implicit and explicit integration methods when the absolute nodal coordinate formulation is used, two integration methods are examined in this investigation. The first method used (HHT-I3) is the implicit Hilber-Hughes-Taylor method modified to handle Index 3 differential-algebraic equations (Negrut et al., 2007). The second method is the explicit Adams-predictor-corrector method, which has a variable order and variable step size (Shampine and Gordon, 1975). These two different integration methods require the use of two fundamentally different solution procedures. Unlike HHT-I3, the explicit integration method requires the identification of the system degrees of freedom and the associated state equations. The formulations and solution procedures used with the two integration methods employed in this investigation are discussed. Numerical examples are presented in order to compare the performance of the implicit and explicit integration methods. The results obtained in this study show that in the case of very flexible structures, where the effect of the ANCF coupled deformation modes can be significant, there is no significant difference between the CPU times of the implicit and explicit integration methods. In this case explicit

integration methods can be used. On the other hand, in the case of very stiff structures in which the ANCF coupled deformation modes are associated with very high frequencies, there is a significant difference between the CPU times of the two methods. The implicit HHT-I3 method, because of its numerical damping properties, can be much more efficient as compared to the explicit ADAMS method.

10. Acknowledgements

This research was supported by the Army Research Office, Research Triangle Park, and the International Program of the National Science Foundation. This financial support is gratefully acknowledged.

References

1. Brenan, K.E., Campbell, S.L., and Petzold, L.R., 1989, *Numerical Solution of Initial-Value Problems in Differential-Algebraic Equations*, North-Holland, New York.
2. Dmitrochenko, O. N. and Pogorelov, D. Y., 2003, "Generalization of Plate Finite Elements for Absolute Nodal Coordinate Formulation", *Multibody System Dynamics*, 10, no. 1: 17-43.
3. García-Vallejo D., Mayo J., Escalona J. L., Domínguez J., 2004, "Efficient Evaluation of the Elastic Forces and the Jacobian in the Absolute Nodal Coordinate Formulation", *Journal of Nonlinear Dynamics*, Vol. 35 (4) , pp. 313-329.
4. Garcia-Vallejo, D., Escalona, J. L., Mayo, J. and Dominguez, J., 2003, "Describing Rigid-Flexible Multibody Systems Using Absolute Coordinates", *Nonlinear Dynamics*, 34, no. 1-2: 75-94.
5. Hilber, H. M., Hughes, T. J. R., Taylor, R. L., 1977, "Improved Numerical Dissipation for Time Integration Algorithms in Structural Dynamics", *Earthquake Engineering and Structural Dynamics*, Vol. 5, pp. 283–292.
6. Hussein, B., Sugiyama, H., and Shabana, A.A., 2007, "Coupled Deformation Modes in the Large Deformation Finite Element Analysis: Problem Definition", *ASME Journal of Computational and Nonlinear Dynamics*, Vol. 2 (2), pp. 146 - 154.
7. Negrut, D., Rampalli, R., Ottarsson, G., Sajdak, A., 2007, "On an Implementation of the Hilber-Hughes-Taylor Method in the Context of Index 3 Differential-Algebraic Equations of Multibody Dynamics", *Journal of Computational and Nonlinear Dynamics*, Vol. 2 (1), Jan. 2007, pp. 73-85.
8. Newmark, N.M., 1959, "A Method of Computation for Structural Dynamics", *Journal of Engineering Mechanics Division*, ASCE, pp. 67-94.
9. Omar, M. A., Shabana, A. A., 2001, "A Two-Dimensional Shear Deformation Beam for Large Rotation and Deformation", *Journal of Sound and Vibration*, Vol. 243 (3), 565-576.

10. Schwab A. L., Meijaard J. P, 2005, “Comparison of Three-Dimensional Flexible Beam Elements for Dynamic Analysis: Finite Element Method and Absolute Nodal Coordinate Formulation”, *Proceedings* of ASME *International* Design *Engineering Technical Conferences and Computers and Information in Engineering Conference - DETC2005*, September 24-28, 2005, Vol. 6 (B).
11. Shabana, A.A., 2001, *Computational Dynamics*, Second Edition, John Wiley & Sons.
12. Shabana A. A., 2005, *Dynamics of Multibody Systems*, Third Edition, Cambridge University Press.
13. Shampine L. F., Gordon M. K., 1975, *Computer Solution of Ordinary Differential Equations*, W.H. Freeman, San Francisco.
14. Sopanen, J. T. and Mikkola, A. M., 2003, “Description of Elastic Forces in Absolute Nodal Coordinate Formulation”, *Nonlinear Dynamics*, 34, no. 1-2: 53-74.
15. Takahashi, Y., and Shimizu, N., 1999, “Study on Elastic Forces of the Absolute Nodal Coordinate Formulation for Deformable Beams,” Proceedings of ASME International Design Engineering Technical Conferences and Computer and Information in Engineering Conference, Las Vegas, NV.
16. Yoo, W.S., Lee, J.H., Park, S.J., Sohn, J.H.. Pogorelov, D., and Dimitrochenko, O., 2004, “Large Deflection Analysis of a Thin Plate: Computer Simulation and Experiment”, *Multibody System Dynamics*, Vol. 11, No. 2, pp. 185-208.

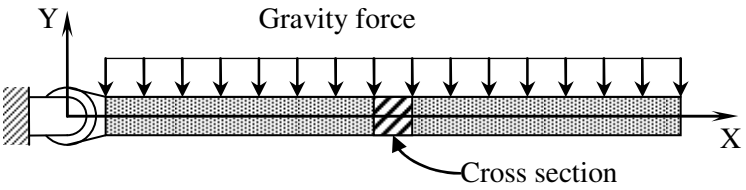

Figure 1. Flexible pendulum initial configuration.

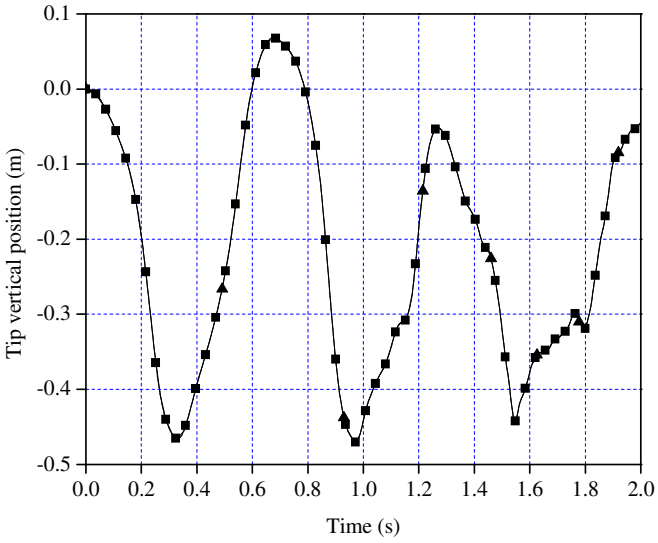

Figure 2. Vertical position of the beam tip ($E=2\times10^5$ N/m^2) (—■—, ADAMS method; —▲—, HHT-I3 method).

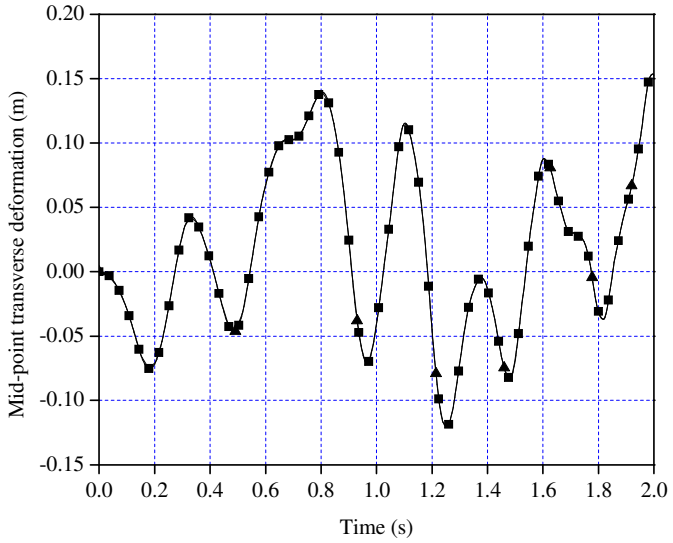

Figure 3. Mid-point transverse deformation ($E=2\times10^5$ N/m^2) (—■—, ADAMS method; —▲—, HHT-I3 method).

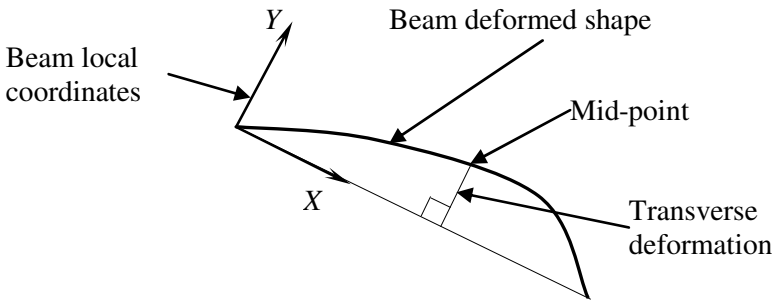

Figure 4. Mid-point transverse deformation.

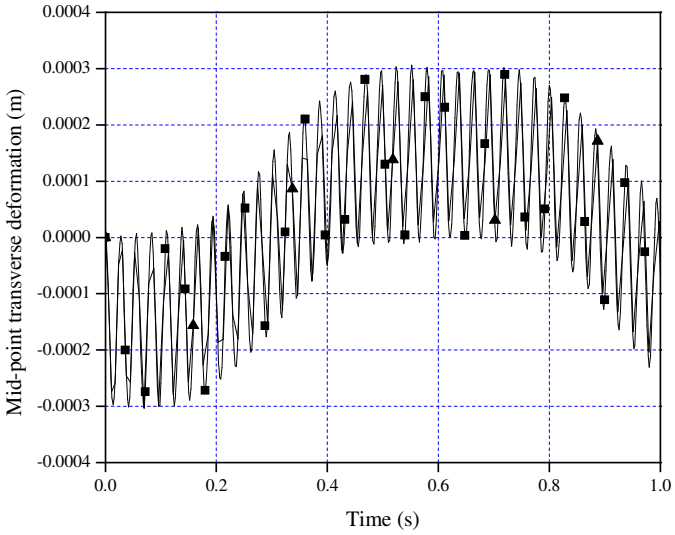

Figure 5. Mid-point transverse deformation (E= 2×10^{8} N/m^2) (—■—, ADAMS method; —▲—, HHT-I3 method).

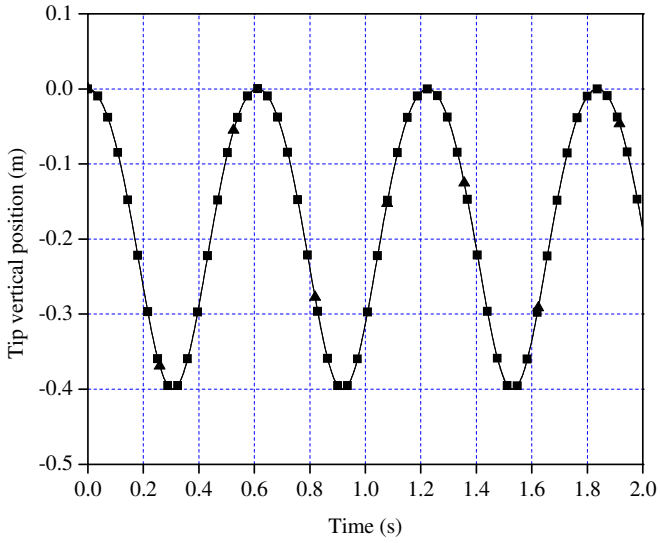

Figure 6. Vertical position of the beam tip (E= 2×10^{11} N/m^2) (—■—, ADAMS method; —▲—, HHT-I3 method).

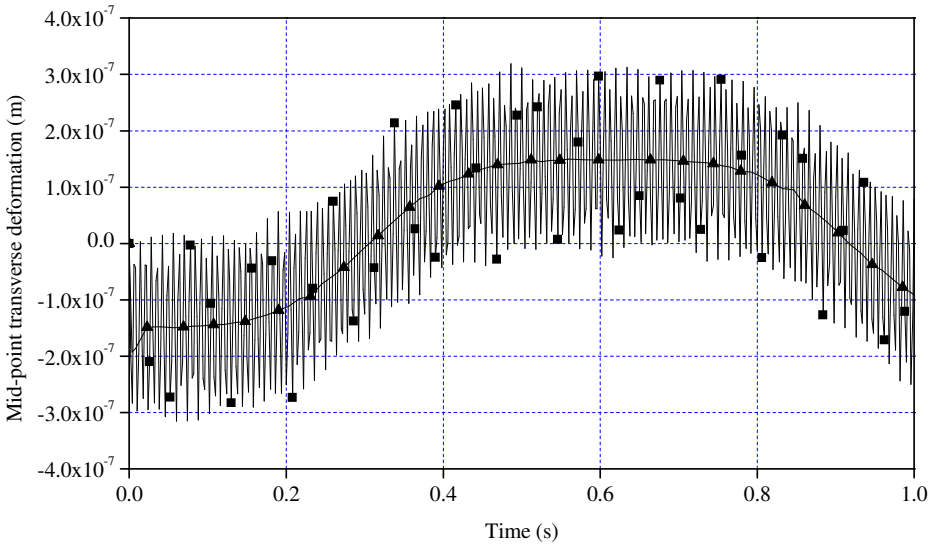

Figure 7. Mid-point transverse deformation (E= 2×10^{11} N/m^2) (—■—, ADAMS method; —▲—, HHT-I3 method).

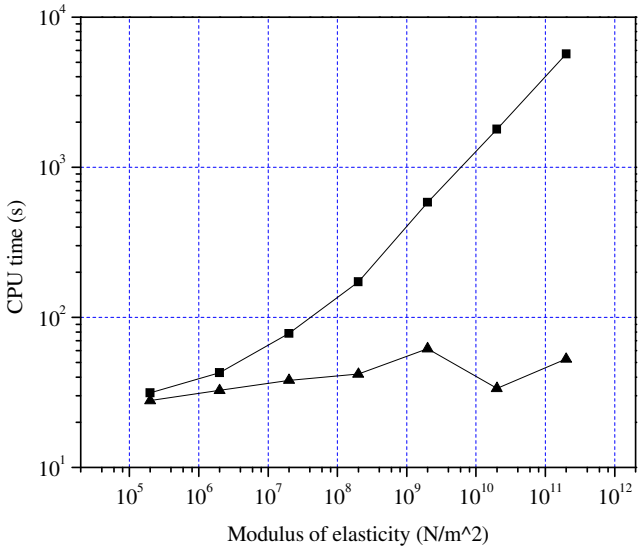

Figure 8. CPU time versus modulus of elasticity (—■—, ADAMS method; —▲—, HHT-I3 method).